google.org

RE<C: Heliostat Wind Tunnel Experiments

Overview

Static wind loading of heliostats, including the forces and moments applied by steady wind, have a strong influence on the design of heliostat components. Wind load simulations can determine how compliant structural components will be before reflector deformation occurs (resulting in a loss of reflected energy) or structural failure happens. Understanding the aerodynamic behavior and loading of our heliostat design enabled systems to be designed while reducing the cost of the heliostat damage and failure.[1]

We performed a series of wind tunnel experiments to gather information on the aerodynamic loads on heliostats and estimate load conditions throughout a typical operational envelope. Scale models were built and subjected to aerodynamic conditions similar to those in the real world to approximate the loads both on an isolated heliostat and a heliostat surrounded by other heliostats in a field.

We also evaluated potential wind mitigation strategies using flow visualization studies. One of our most interesting results was that porous fences provided better wind resistance than solid walls. Multiple fences are even better, but their construction comes at an additional cost.

Our wind tunnel studies are intended to augment and expand on previous studies using modern

[1] Significant material exists on the topic of aerodynamic loading on heliostats, much of which was published by Colorado State University and the Solar Energy Research Institute. See Peterka, et. al., 1986, Peterka, et. al, 1987, and Peterka, et. al. 1988.

day equipment. Most of the relevant published work in the field is in excess of 20 years old. This work is not fully comprehensive nor all-encompassing. For a more complete set of charts, graphs and data sets, please see the Appendix. For broader information on our wind studies on heliostats and our design approach to studying wind, please see our wind mitigation overview.

Experiment Setup and Approach

Facilities

NASA Ames is a natural partner for collaboration for this aerodynamic behavior study. Their facility is very close to Google in Mountain View, CA, and NASA houses some of the world's leading aerodynamicists and test facilities, giving us access to a wealth of information and experience.

NASA Ames Fluid Mechanic Laboratory

The wind tunnel we used at the Fluid Mechanics Laboratory is an open loop indraft wind tunnel. This type of tunnel uses suction at the tunnel exit to create flow through the test section. A set of filters and screens is placed at the tunnel inlet to eliminate any disturbances in the ambient air and to straighten out the incoming airflow. A standing shock wave is maintained at the tunnel outlet to isolate flow disturbances in the test section from the suction manifold. This wind tunnel supports dynamic pressure (Q) from 0.28-1.53 kPa (8-32 psf) and has provisions to support uniform flow and atmospheric boundary layer flow conditions.

The tunnel test section is 0.82m tall x 1.21m wide and has a usable length of approximately 1.21m. Centered in the test section floor is a 0.82m rotary table section driven by a controllable geared motor. This section is capable of rotating 360 degrees to provide various wind incidence angles on any models attached to it. We used this table extensively during our wind tunnel testing. Typically, the table rotates counter clockwise when viewed from above.

Data Acquisition

NASA Ames has a built-in DAQ (Data Acquisition) system that is used to gather:

- Wind conditions in tunnel (velocity, temperature, density, relative humidity, etc)
- Forces and moments measured by a 6-axis load balance (model Task EZ3)

The balance is capable of recording all 6 axis data at 200 Hz (with 0.01% accuracy), however this high frequency data is not very useful for scale model tests[2]. Therefore the DAQ software (LabVIEW) records the measured loads for 9 seconds and then reports out the mean value from that 9 second sample.

The balance is typically secured to the rotating table of the test section and thus rotates with the table. The balance is secured to the desired model of interest either directly or through a connection rod. Both the wind flow characteristics and the data collection abilities of the wind tunnel are shown in the following graphs.

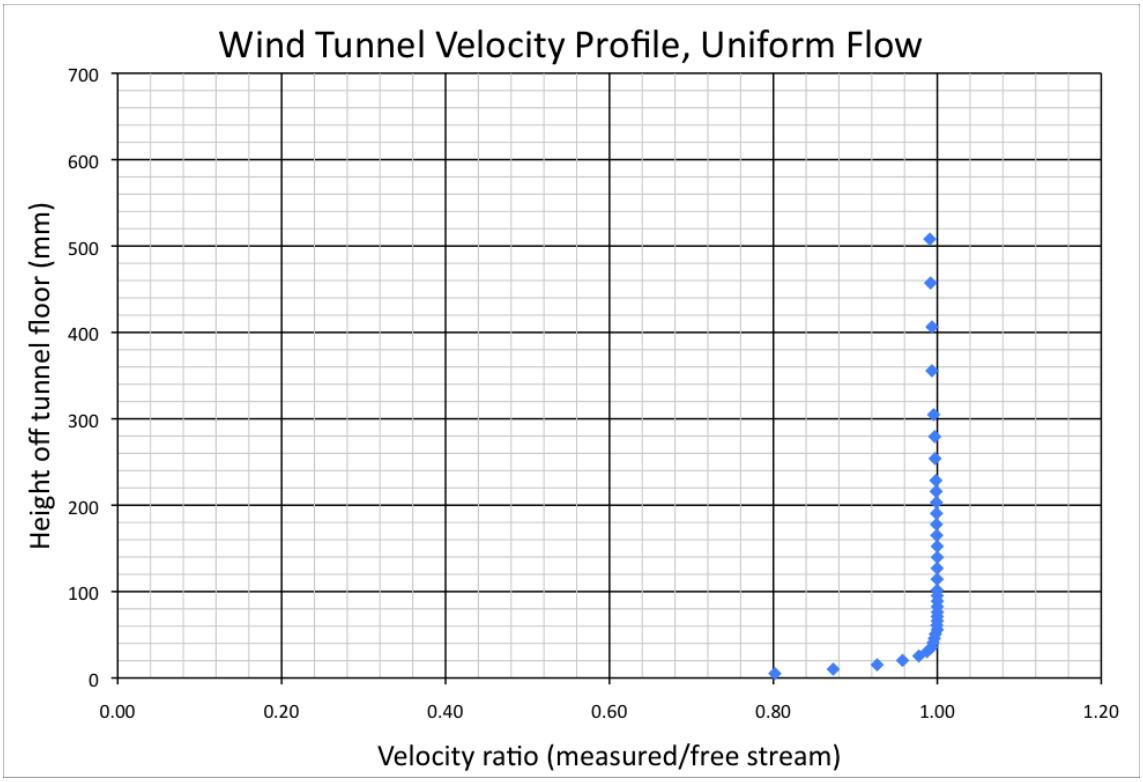

Uniform flow velocity profile

[2] The fluctuations of the load parameters is not reported. The dynamics of the system (e.g. stiffness, the natural frequency) do not scale with size because structural stiffness is dependant on material properties. Read about Young's modulus for more information.

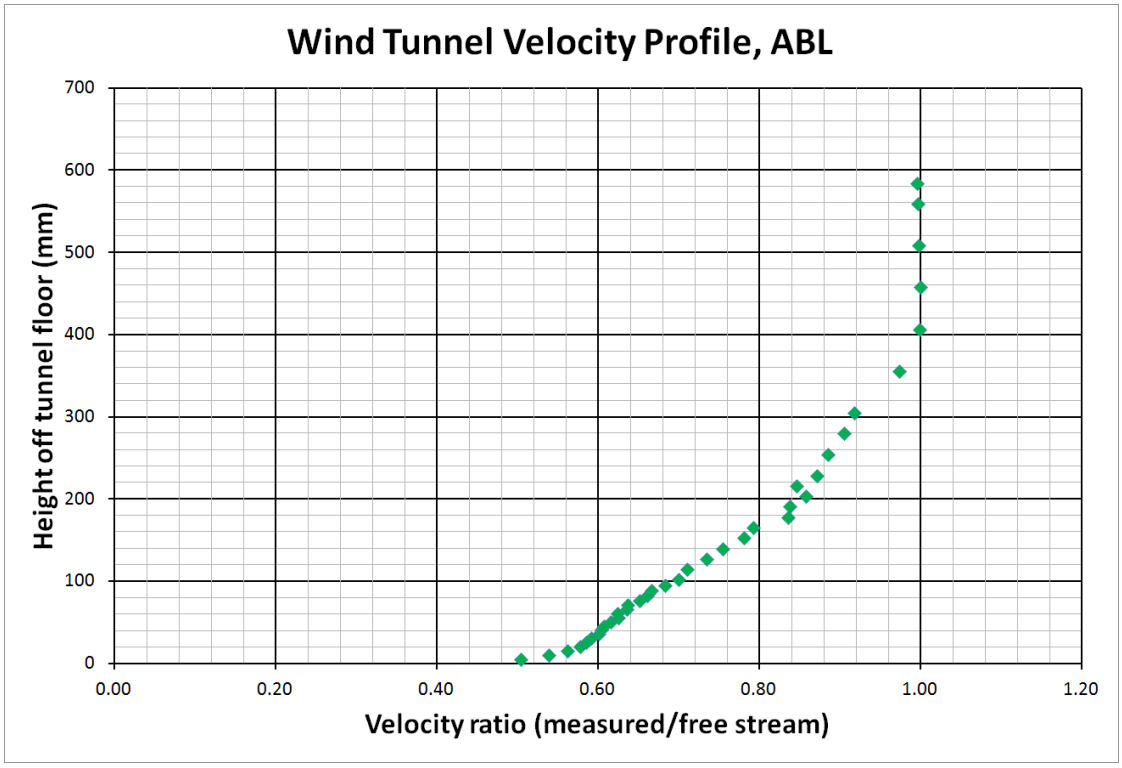

Atmospheric boundary layer velocity profile

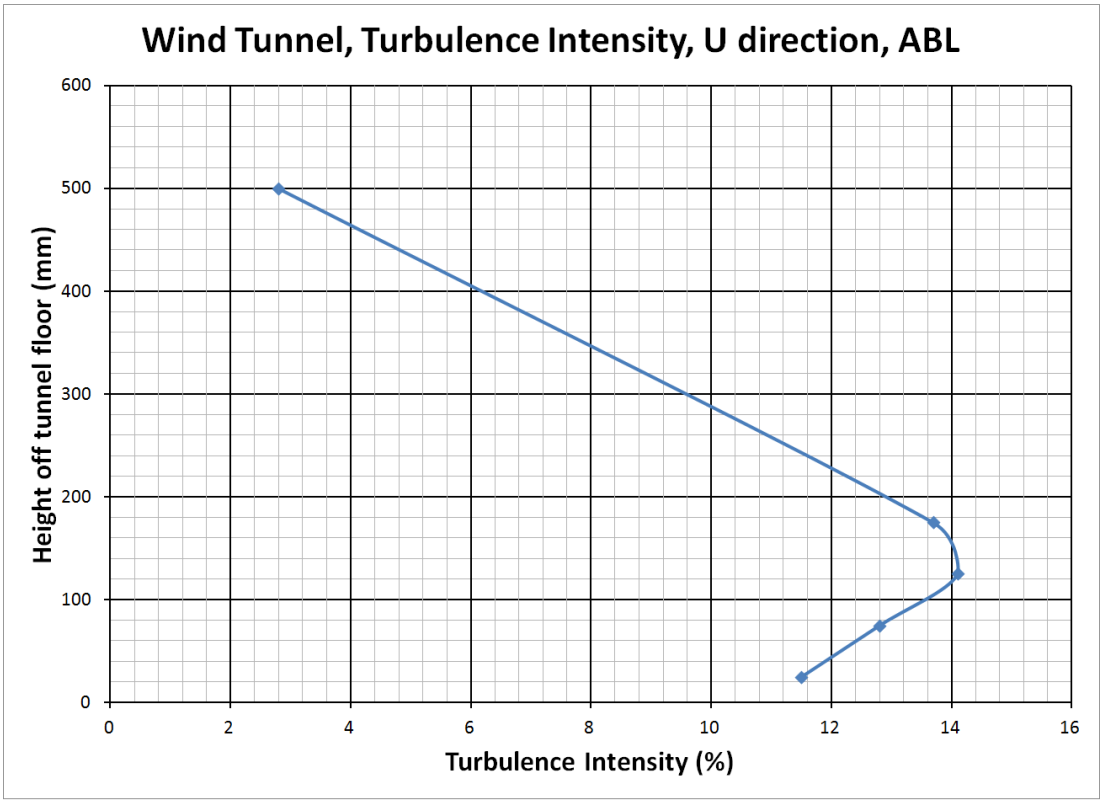

Atmospheric boundary layer turbulence intensity profile

Calculating Loads

Aerodynamic loads on heliostats are determined by the:

- Heliostat geometric size and shape
- Fluid properties (velocity, density) of wind

For a heliostat installed at a CSP site, the geometric size and shape are set, unchanging properties. However, the fluid properties can fluctuate, most notably the wind velocity. Therefore, relevant results are provided as force or torque coefficients, rather than actual forces or torques. These coefficients are dimensionless and can then be used (along with the relevant wind properties) to estimate the actual forces and torques experienced by full-size heliostats using the following equations:

$$F = C_f * \frac{1}{2} * \rho * V^2 * A \quad \text{(EQN 1)}$$

$$M = C_m * \frac{1}{2} * \rho * V^2 * A * L_{ref} \quad \text{(EQN 2)}$$

Where:

- $F\ (or\ M) =$ Force [N] or Moment [N-m]
- $C_f\ (or\ C_m) =$ Force or Moment coefficient (respectively)
- $\rho =$ Air density at given air temperature [kg/m3]
- $V =$ Air velocity (wind) [m/s]
- $A =$ Frontal Area [m2]
- $L_{ref} =$ Reference Length [m]

Nomenclature and Coordinate Systems

In order to interpret our results, a quick discussion on the coordinate system and nomenclature we used is required. The nomenclature we used is described below.

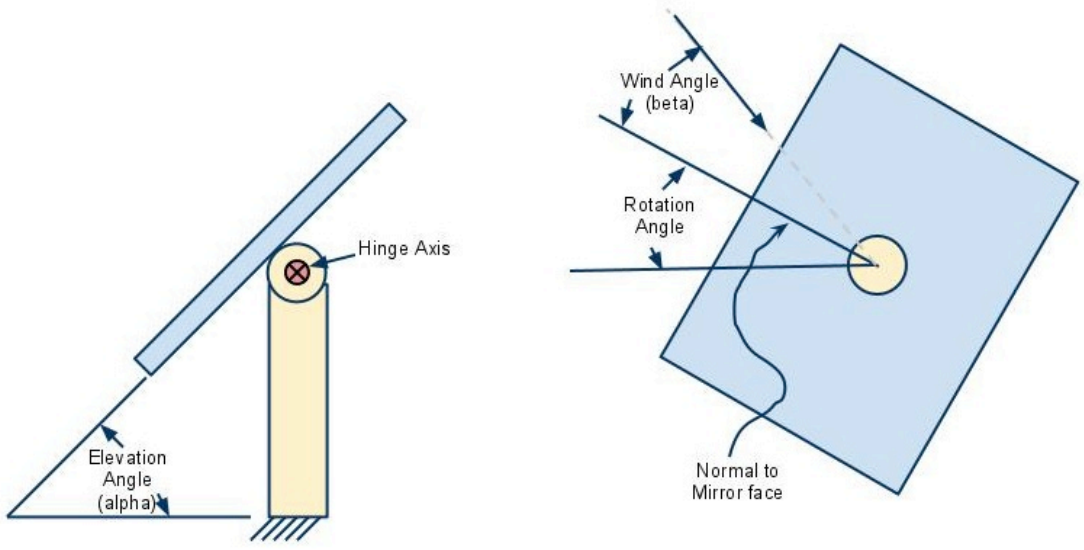

Example heliostat with relevant parameters

Elevation Angle (α):	The angle between the mirror plane and the ground surface (assuming the ground is perfectly horizontal). 0^o is when the planes are parallel, 90^o is when the planes are orthogonal
Wind Angle (β):	The angle between the nominal wind direction and the mirror normal, projected on the ground. This is not Azimuth Angle.
Mirror Centroid:	The volumetric centroid of the flat plate of the mirror (Coordinate system origin located here)
Hinge Axis:	The axis about which elevation angle is provided
Mirror Normal:	A line projected from the mirror centroid, orthogonal to the mirror plane
Heliostat Centerline (HCL):	The vertical distance from the ground to the hinge axis, also called HCL

The wind tunnel experiments we performed were part of a larger set of analyses that included CFD (Computational Fluid Dynamics), as well as atmospheric wind load measurement and analysis. While each analysis has a preferred coordinate system, in order to compare results from one analysis to another, we had to select a common coordinate system.

We chose a coordinate system that was convenient for the CFD analysis as the common coordinate system for all our wind studies. CFD analysis uses a coordinate system that has its origin at the mirror centroid and is aligned with the approaching wind (see the diagram below). Unlike the CFD analysis, the wind tunnel test used at NASA Ames has a coordinate system that is oriented with the heliostat. If the heliostat is aligned directly with the wind, these coordinate systems align. As the alignment changes (if $\beta \neq 0$), the coordinate systems become "out of phase".

A series of equations was used to transform the calculated coefficients from the wind tunnel load balances' coordinate system to the chosen common coordinate system aligned with the wind. The final coefficients as calculated from the wind tunnel are thus designated with a "_CFD" suffix to denote the coordinate system change.

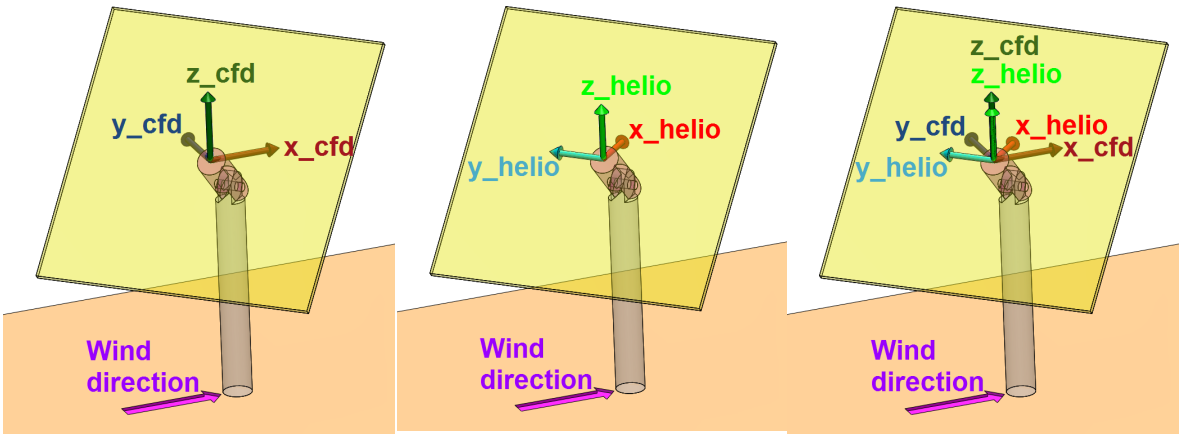

From left to right: CFD coordinate system, heliostat coordinate system, and out of phase coordinate systems, all shown at heliostat orientation $\alpha = 45^o$, $\beta = 45^o$

The final coordinate system for the reported coefficients is represented in the graphic below. Coefficients are discussed in detail in the Coefficient Summary and Reference.

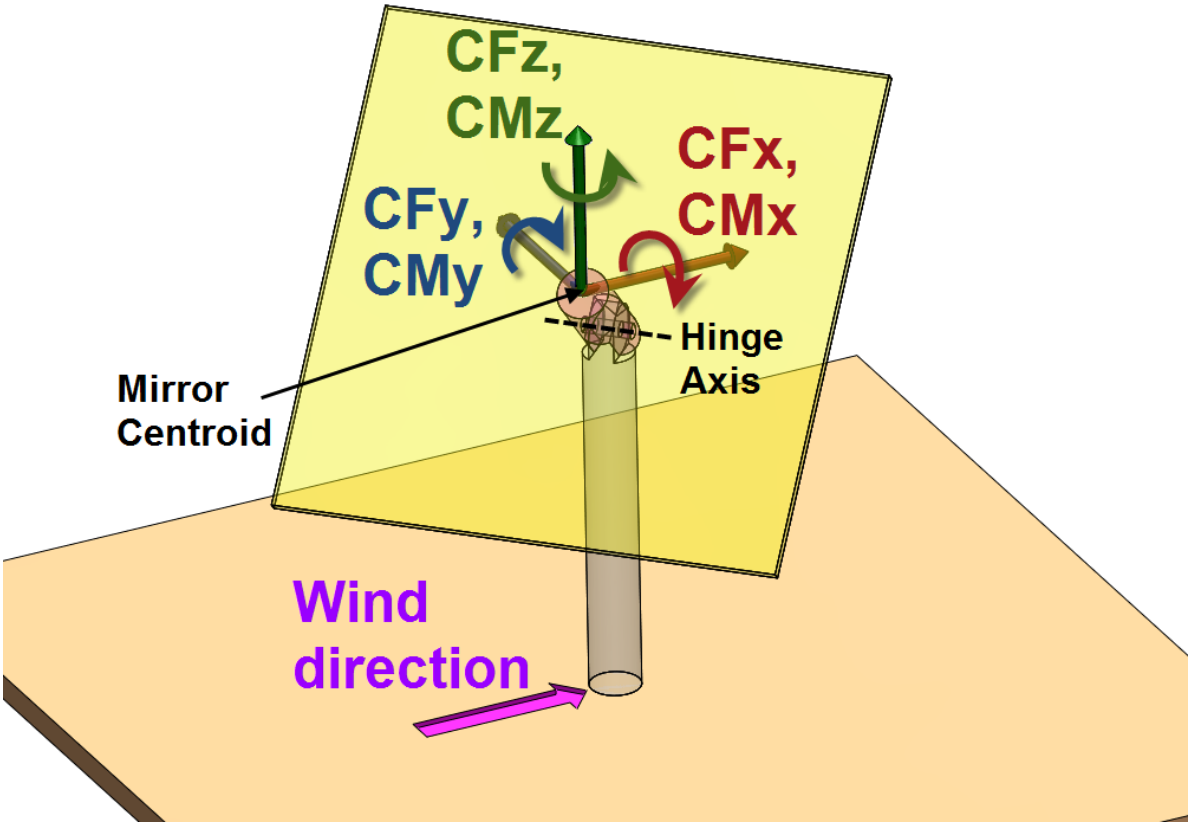

Coordinate system used, heliostat shown here at α = 45°, β = 45°

Single Heliostat Experiments

The first set of wind tunnel experiments were designed to identify the aerodynamic loads on a single isolated heliostat. This experiments needed to accomplish three goals:

1. Validate the setup of the wind tunnel, model, and data acquisition system against known values.
2. Collect load information for CFD model validation.
3. Collect load information to serve as the comparison basis for heliostat field tests.

A scale model of our heliostat was constructed (model reflector size = 200mm x 200mm x 5mm, HCL = 150mm) and subjected to uniform[3] flow conditions and turbulent boundary layer flow conditions.

[3] Truly uniform flow very rarely exists in nature but is useful in early testing to check the integrity of the model setup and to validate reported load coefficients against theoretical calculated load coefficients.

Single heliostat model in wind tunnel (shown here behind fence)

This first set of experiments consisted of the following:

- Wind tunnel setup and coefficient validation
- Uniform Flow load analysis
- Atmospheric Boundary Layer load analysis
- 1.5 aspect ratio reflector load analysis
- Single heliostat load mitigation tests (upstream fence, hemispherical backed mirror)

The atmospheric boundary layer (ABL) was created in the wind tunnel using a series of turbulence generators. This consists of three distinct devices: spires (to create vertical tornado type vortices), dragon teeth (to create rolling, tumbling vortices), and a fence (to completely disturb/trip up the flow nearest the ground).

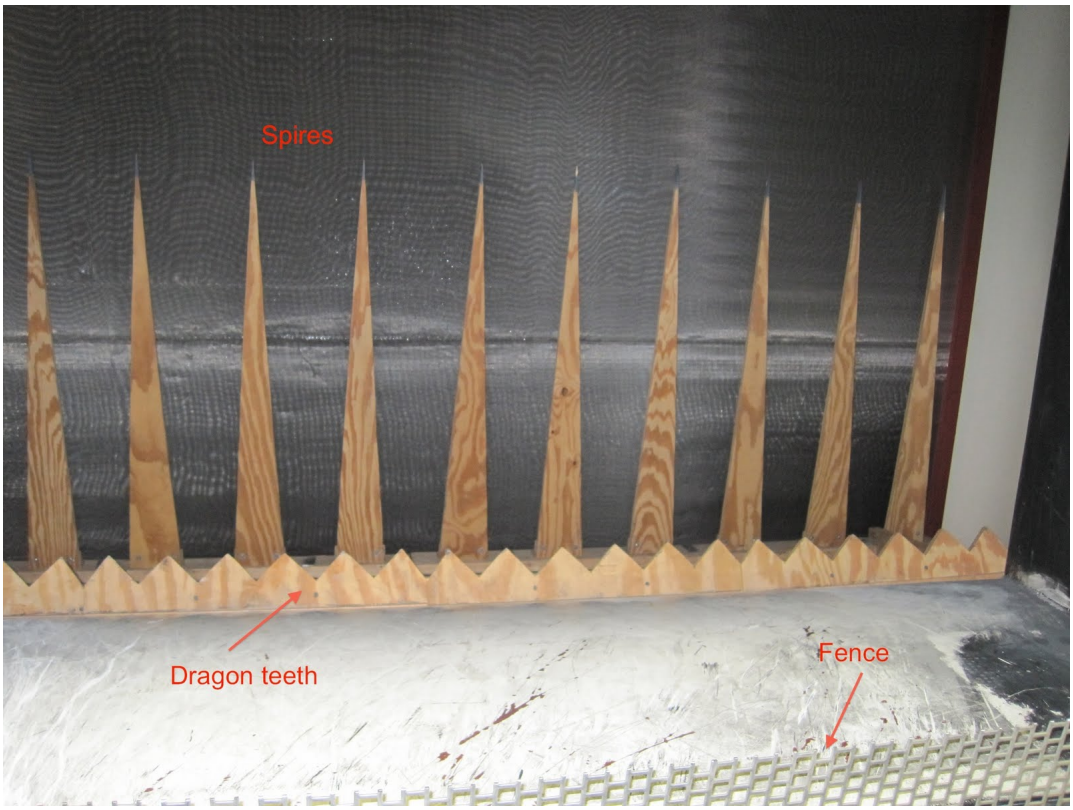

NASA Ames Atmospheric Boundary Layer generator

Test conditions were as follows:

- Wind Speed = 18.2 m/s (60 ft/s) (41 MPH)[4]
- Air Temperature = 23 C (74º F)
- Air Density = 1.20 kg/m^3 (14.85 psia, as reported from tunnel conditions)
- Elevation angles (α) tested: 90, 75, 60, 45, 35, 30, 25, 15, 0 degrees
- Wind incidence angles (β) tested: 0 - 360 in 5 degree increments

Single Heliostat Experiment Results

To validate our results and establish a baseline, we use the level of drag on a classic flat plate reflector as a point of comparison. According to textbooks and industry references, the accepted drag coefficient (C_D) for a flat plate perpendicular to the flow is C_D = 1.28. The measured drag coefficient was C_{D_CFD} = 1.29, matching very well with the theoretical value.

Using a simple experimental setup also allowed us to verify our CFD model. Building a CFD scenario similar to the NASA wind tunnel, we found that the CFD modeled loads matched reasonably well (though not perfectly) with our wind tunnel data, improving our confidence in using CFD for other analyses.

[4] This velocity does not allow for Reynolds number matching between wind tunnel test conditions and real world operational conditions, however this was the maximum permissible velocity for the model construction used during these tests. Additionally, it was shown that coefficients do not vary significantly with velocity in this set of experiments, which validates work by Peterka, et.al 1987

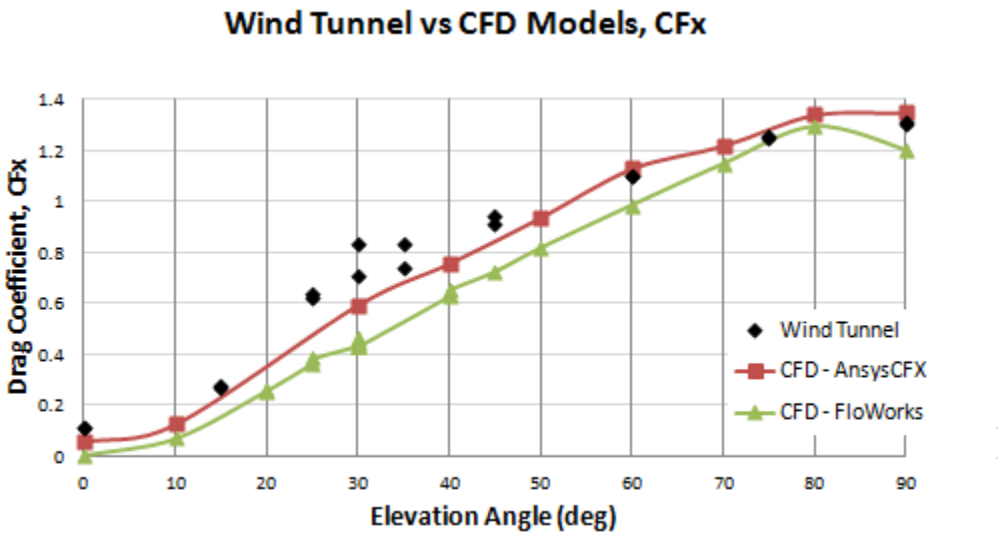

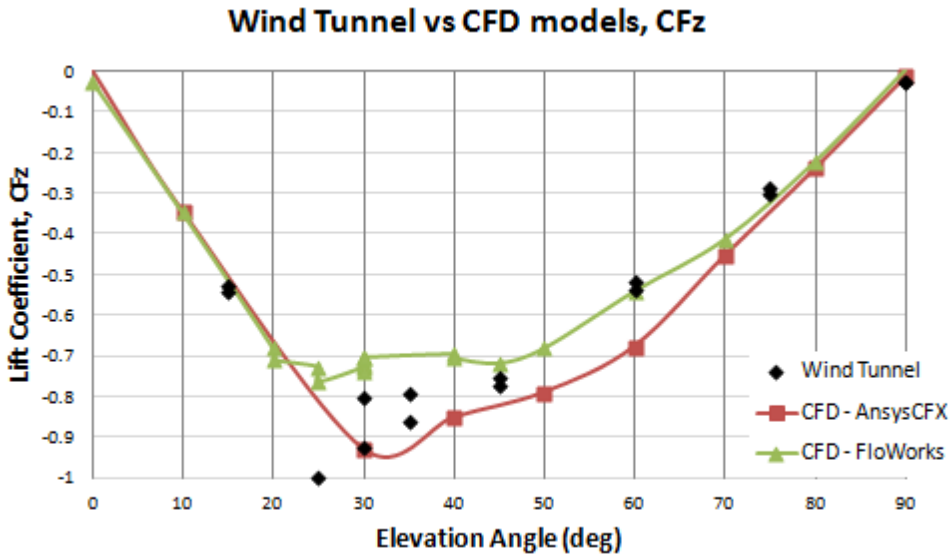

Comparison of wind tunnel and CFD modeling results

While these tests correlated well with the expected *trends* based on previously published work, the magnitude of the measured coefficients varied, one example is shown below, comparing our wind tunnel results with published results by Peterka, et. al.

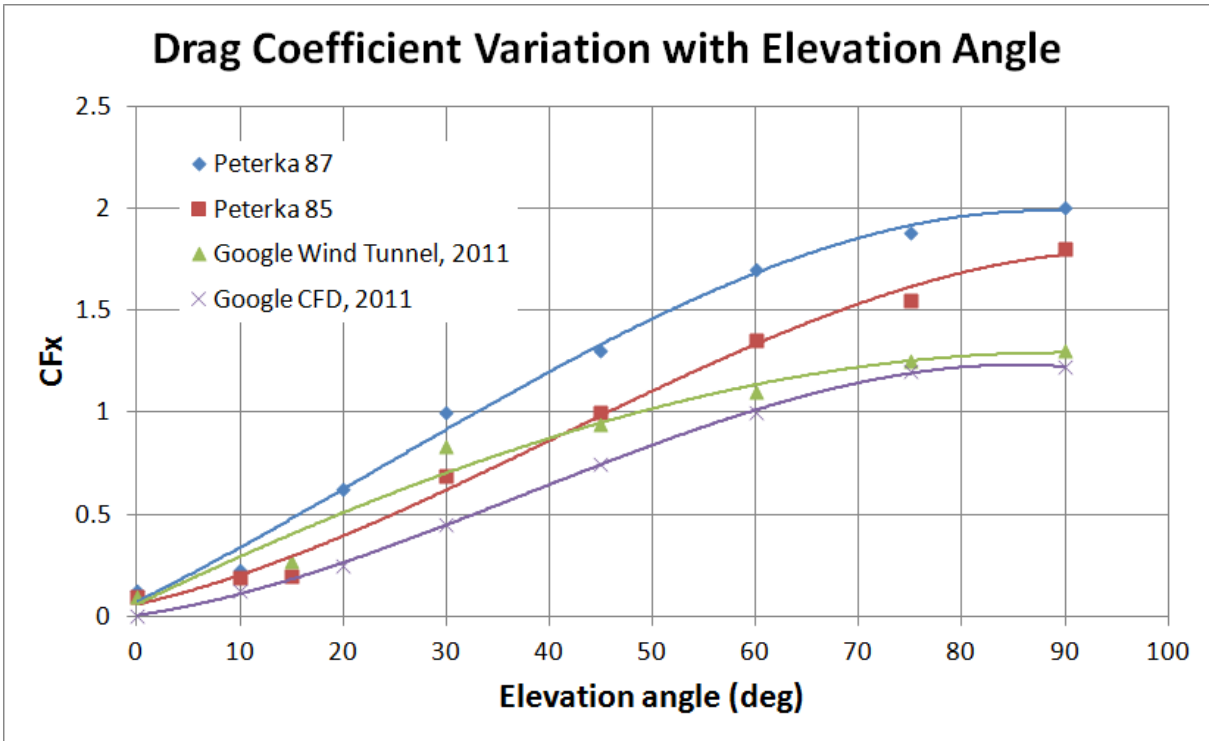

Comparison of measured wind tunnel parameters vs published literature

We tested a single heliostat under uniform flow conditions as part of the wind tunnel setup and validation. One interesting phenomena that occurred during the uniform flow testing was the appearance of “vortex lift” on the heliostat at certain combinations of α and β. Vortex lift sometimes occurs in a wing system where the angle of incidence relative to the wind is such that the vortices shed from the body dramatically increase the lift on the body. In this case, a model heliostat reflector looks very similar to a wing.

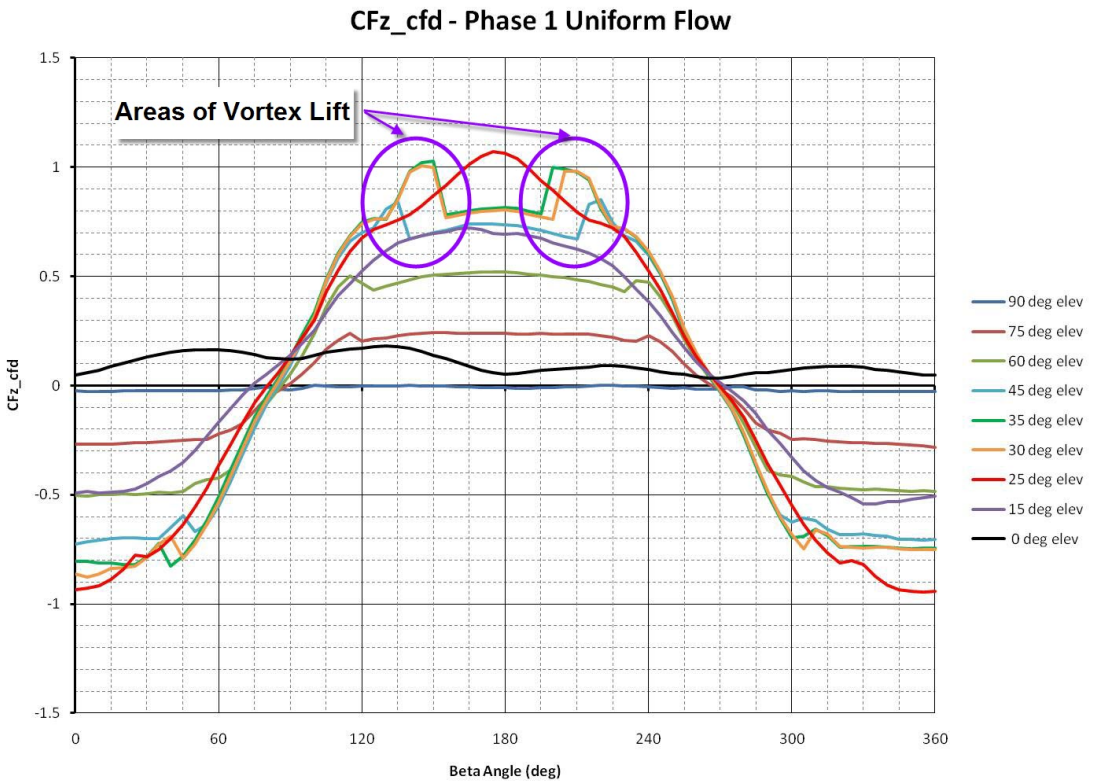

Vortex lift phenomenon observed under uniform flow

The vast majority of the testing was performed under ABL conditions. We observed that compared to uniform flow, reduction in loads of up to 50% occurred under ABL conditions. The reduction in loads (in a single direction) is due to energy in the fluid being scattered and directed in multiple directions, as opposed to being pointed in a single direction. For the full set of test results, see the Wind Tunnel Experiment Appendix.

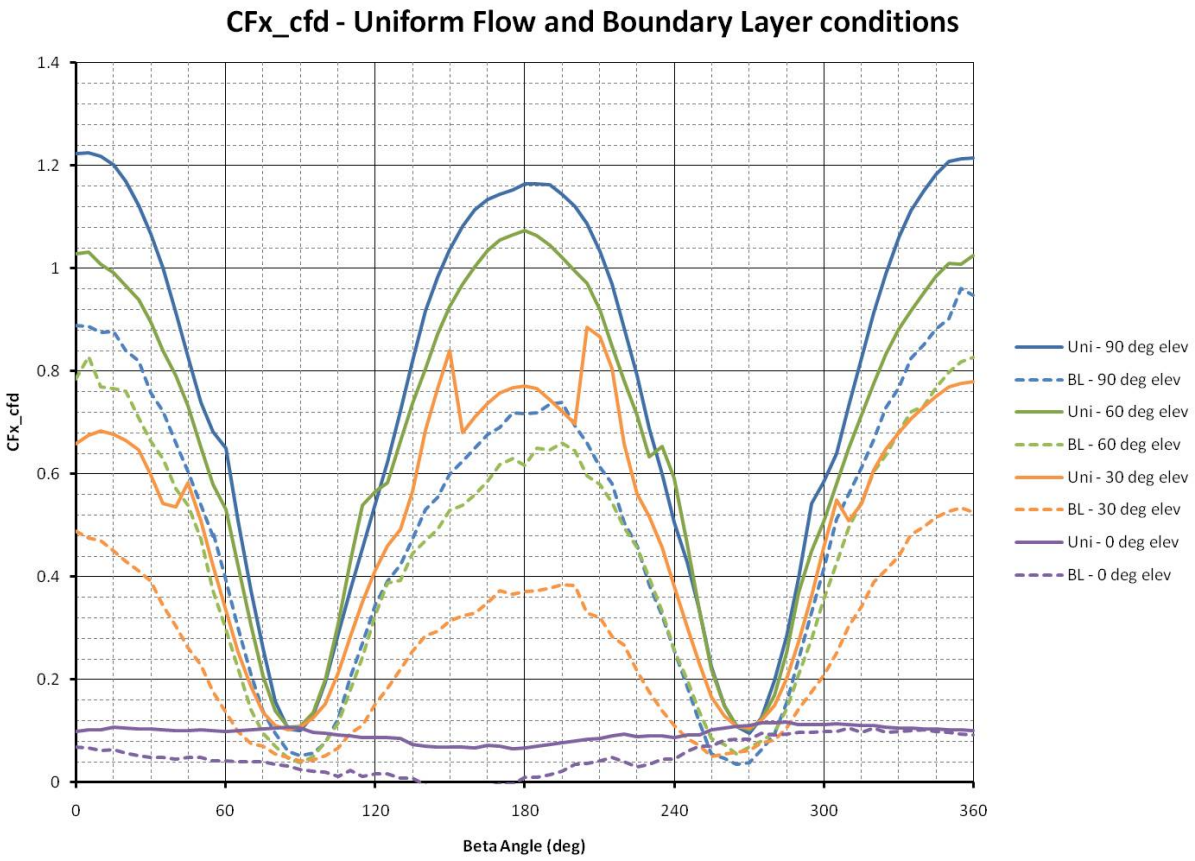

Comparison of CFx parameter for Uniform and Boundary layer test conditions

We also performed a test with a single non-square heliostat. Most heliostats used in tower-CSP fields use square reflectors, but a few designs use rectangular reflectors. Our candidate heliostat design used a rectangular reflector, so it was important to understand if this changes any of the wind loading results. We built a reflector model with a 1.5 aspect ratio (reflector size = 150mm x 100mm x 3mm) for wind tunnel testing.

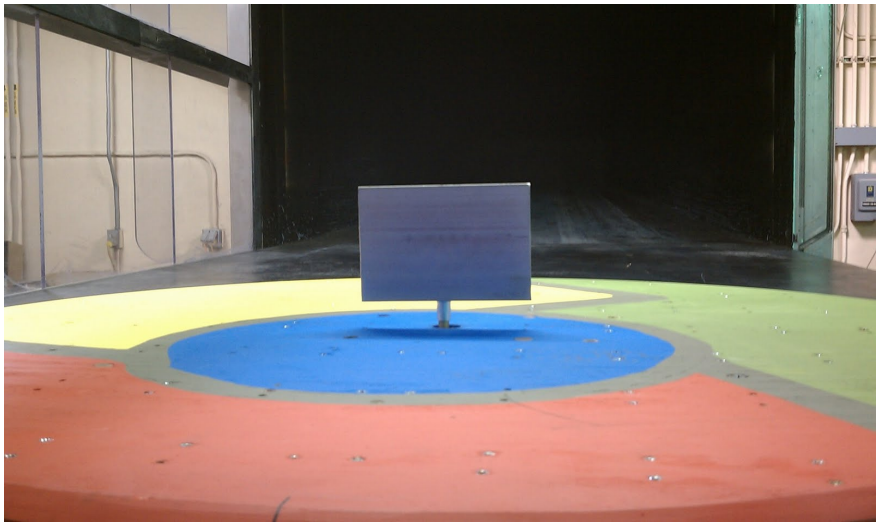

Heliostat model with 1.5 aspect ratio reflector

Compared to the square reflector, no significant difference in the loads on the heliostat were recorded, with the exception of roll moment (CMz). CMz is increased with the larger AR mirror, which is expected as there is more mirror area offset from the heliostat vertical axis. The increase in CMz is about 150%, which corresponds to the difference in aspect ratio.

Heliostat Field Experiments

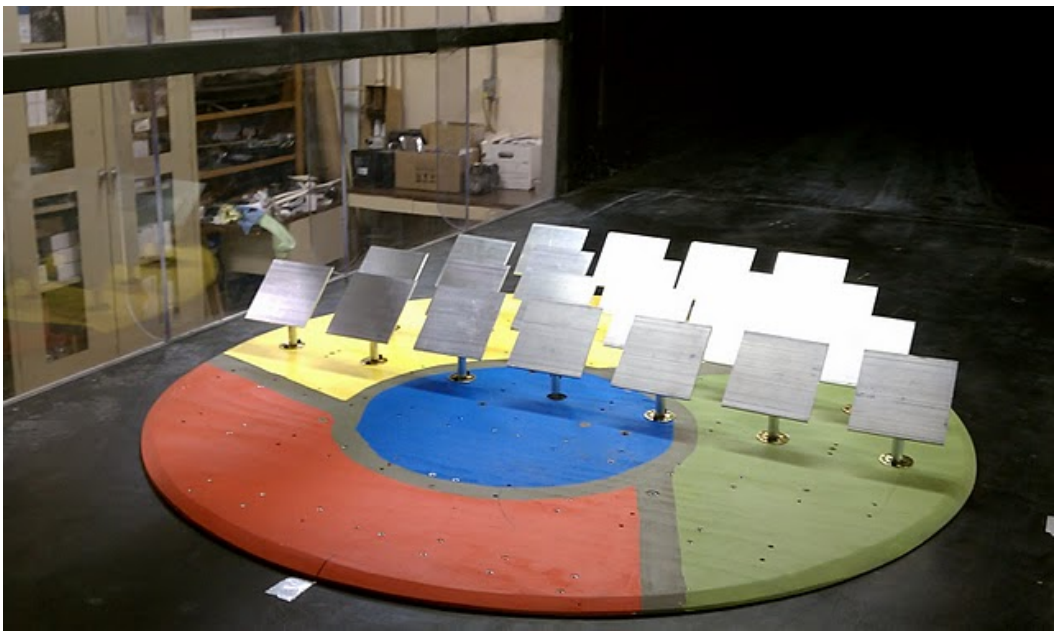

Heliostat field model in wind tunnel

The second set of experiments were design to mesaure the differences between loads on a single isolated heliostat, a heliostat at the edge of a heliostat field, and a heliostat buried four rows deep in the heliostat field. Our qualitative study in the NASA flow visualization chamber informed us that beyond the fourth row, the flow is sufficiently disturbed and the vast majority of the energy from the wind has been absorbed.

A model consisting of 22 square heliostats (reflector size = 100mm x 100mm x 3mm) mounted on an index plate was used in the wind tunnel for our tests. The scale of the model had to be reduced from the single heliostat tests (reflector size = 200mm x 200mm) so that the overall wind tunnel blockage was kept to admissible levels. The index plate (supporting the heliostat models) was attached to the rotating plate in the NASA wind tunnel to provide varying wind incidence angles.

The model was constructed such that one model heliostat was instrumented at all times with the NASA 6-axis load balancer which measured wind load, and the remaining 21 un-instrumented heliostat models (i.e. “dummy” models) were positioned around the instrumented model to simulate various field positions. The instrumented heliostat could be positioned at the edge of the field or mid-field as shown in the diagram below.

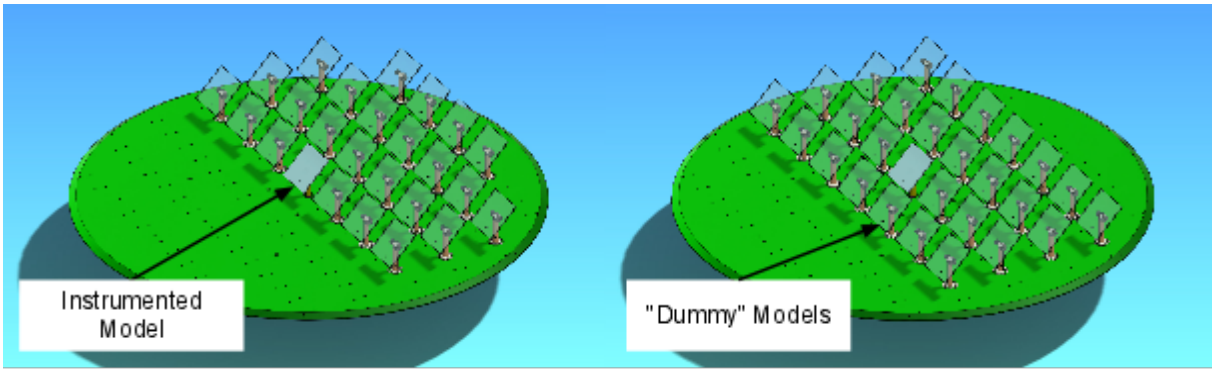

Instrumented model in 1st row Instrumented model in 2nd row

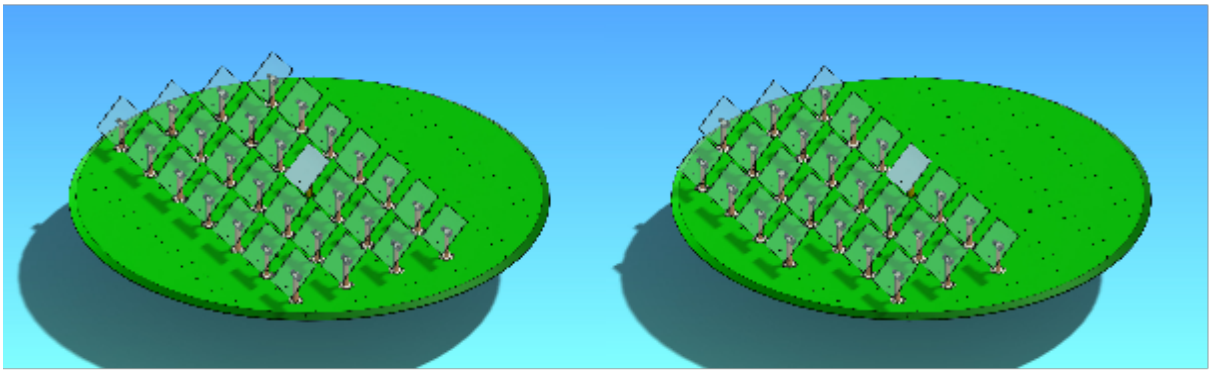

Instrumented model in 3rd row Instrumented model in 4th row

Multiple positions of instrumented heliostat on model

The heliostat field was constructed with a fairly high packing density of 50% (to approximate our target field packing density of 47%). Packing density is determined by:

$$\frac{(Reflector\,area, m^2)}{(Total\,Field\,area, m^2)}$$

Before examining the observed coefficients, an important aspect of the test and reported results must be made clear. Because the heliostat field was attached to the turntable, a heliostat that begins the test as an "edge heliostat" will change to a "mid-field heliostat" at 180° of rotation. Thus, in a single test run (rotating the index plate 0-360°) we are able to observe the relative loads for a heliostat at the edge and in the 4th row of a field, but this does require accounting for the reversal of elevation angle.

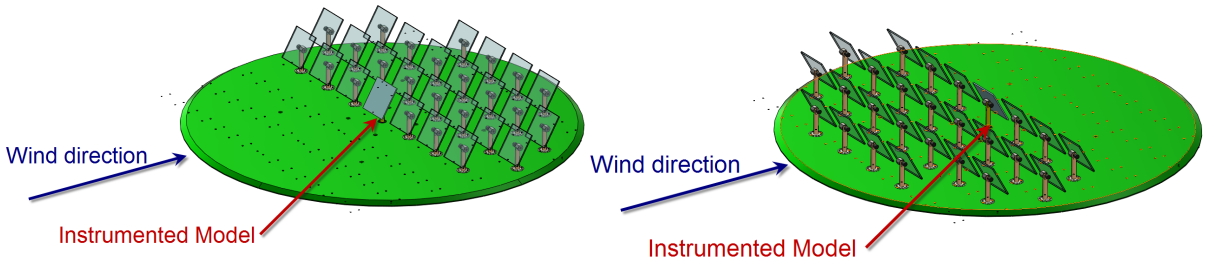

Instrumented heliostat model in 1st row at β=0° (LEFT) and at β=180° (RIGHT)

When reading the data and charts in the Appendix, note that at β=0°, the instrumented model is at one field position (such as the edge in the example above) and at β=180° the instrumented heliostat may be at a different field position (the 4th row in the example above) for a given elevation angle (α).

The tests we performed consisted of the following:

- Smaller model validation (ensuring the coefficients remain the same given a smaller model and different test setup)
- Field position study (edge vs. mid-field heliostats)
- Sparse vs. dense field (25% vs 50% packing densities)

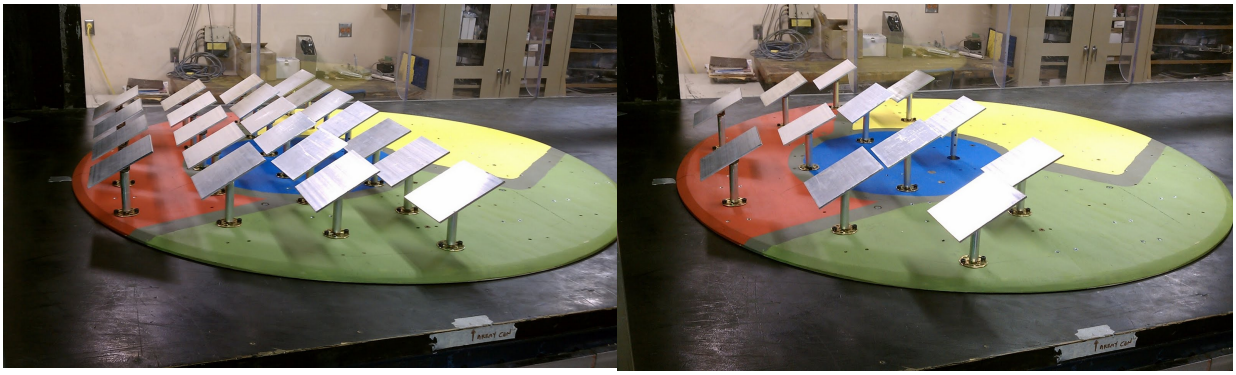

Packing density study, 50% (LEFT), 25% (RIGHT)

Field Experiment Results

Our tests were able to put some quantitative information behind the visual information that observed from our flow visualization testing. The results we found included:

- Heliostats at the edge of a field experience similar load conditions to isolated heliostats (within 10%).
- The 4th row of heliostats experience loads at least 50% less than edge heliostats for nearly all elevation angles (in most cases, the reduction in loads is more significant, as high as 1000%). A majority of this load reduction is observed by the 2nd row of heliostats, which has loads of about 60% of an edge heliostat.

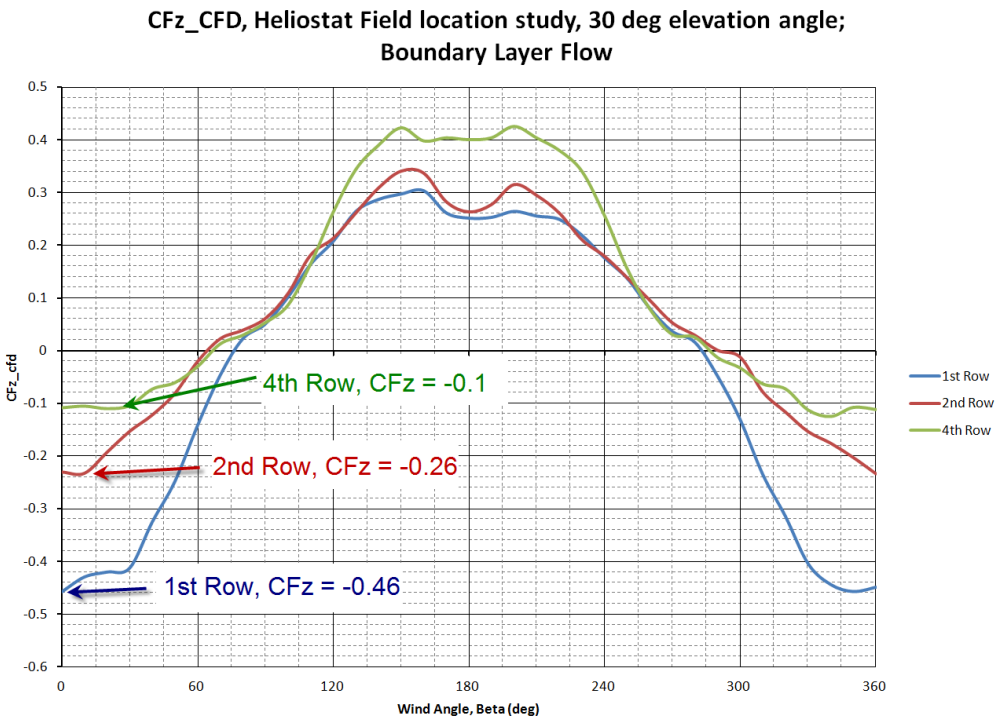

Heliostat wind loads by row

- As expected, a more densely packed heliostat field does a better job providing protection for downstream heliostats than a sparsely packed field. For example, a densely packed field reduces drag loads by ~400% by the fourth row, however a sparsely packed field only reduces drag loads by ~30%.
- While general trends in loads can be approximated, heliostat fields have very complex wind flow patterns, making accurate, repeatable load prediction difficult. Evidence of this is the very "noisy" load plots with changing wind angle, compared to isolated heliostats which have much smoother, more predictable load patterns.

For the full set of test results, see the Wind Tunnel Experiment Appendix.

Mitigation Experiments and Results

We experimented with two types of wind mitigations that may be effective to reduce heliostat aerodynamic loading:

- Individual heliostat specific mitigations (e.g. additional hardware or modifications to each heliostat)
- Field level mitigations

We discussed many ideas and discarded several due to hardware complexity, reliability issues, or after discussing them with aerodynamicists at NASA. However we decided to test a few in the wind tunnel to quantify their effect.

Hemispherical-Backed Heliostat

One thing we suspected is that when the wind incidence angle is approximately at β =180 deg (i.e. wind from directly behind the heliostat), the back of the heliostat structure may create significant drag due the typical complex network of reflector support structure. We proposed shaping a hemispherical dome over the back of the heliostat to reduce this aerodynamic loading.

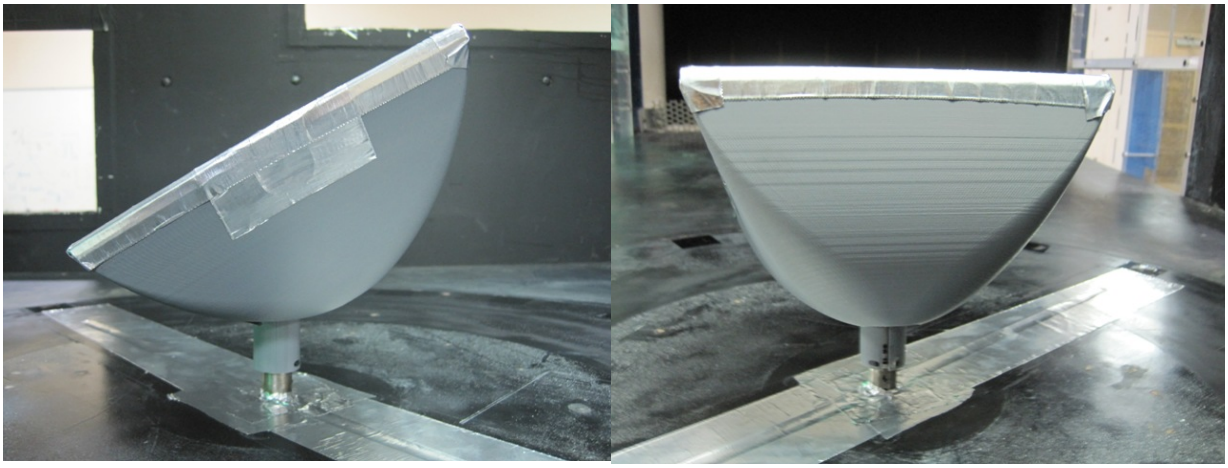

Heliostat model with hemispherical backing

When tested, the hemispherical back reduced the lift loading at β =180^{o} significantly (approximately 6x from the chart below), however it didn't have a significant impact on the remaining load coefficients and therefore probably wouldn't be worth the extra cost of manufacturing, transporting, and installing such a large additional structure on the heliostat, not to mention the additional engineering required for the heliostat frame to support the extra mass.

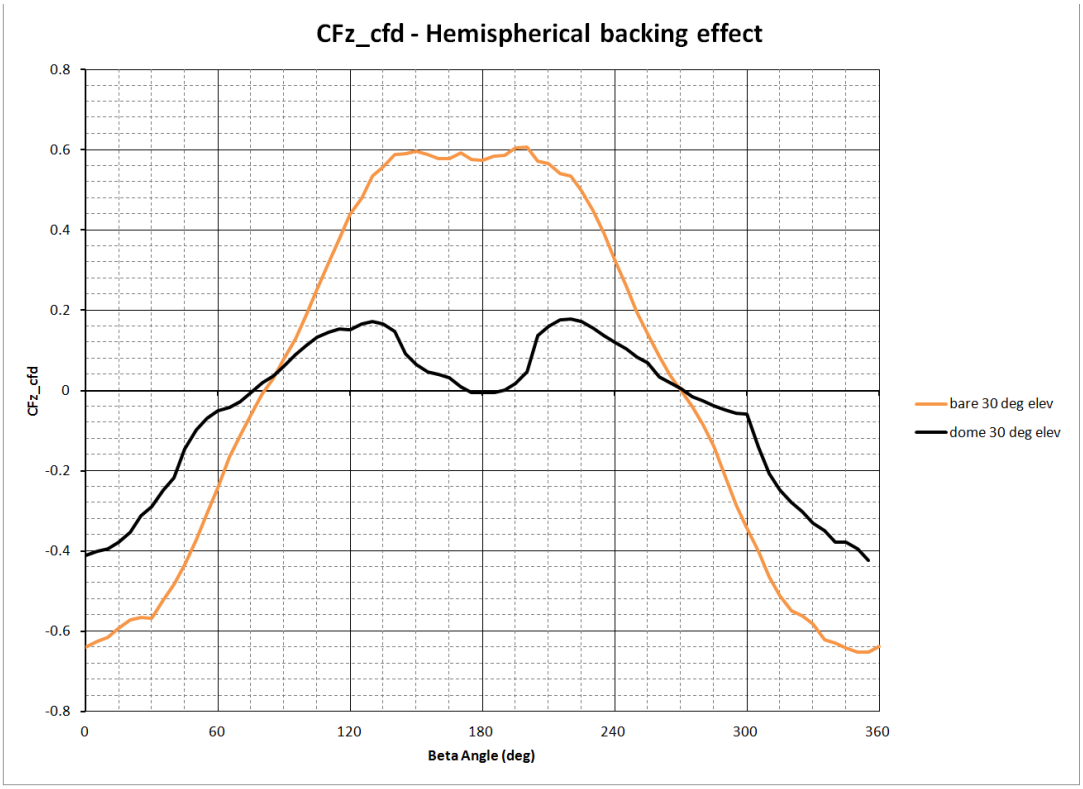

Effect of hemispherical backing on lift coefficient

Fences

Our early wind tunnel experiments and flow visualization studies indicated that fences would have a significant effect on reducing heliostat loads (demonstrated in this short video), so we spent some time quantifying the effect of fences on heliostat aerodynamic loads. We expanded our tests to understand the effect of fence height, fence blockage and the distance between the fence and the heliostats.

Ideally, the fence would be inexpensive to maximize the cost-benefit of the load reduction. Our fence should use as little material as possible. Experiments were run to understand how fence height, fence blockage, and distance between the fence and the heliostats affected the loads.

The tests performed regarding fences included:

- Fence porosity (compare 40%, 46% and 58% open area fences with no fence).
- Fence height (compare 0.75*Hmax[5], 1*Hmax, 1.5*Hmax, 2*Hmax fence heights).
- Fence upstream distance (compare 6.6*H[6] and 10.4*H distances upstream).
- Multiple upstream fences.

[5] Hmax = maximum overall height of a heliostat at any position.

[6] H = heliostat reflector characteristic length, in this case the length of one side of the reflector.

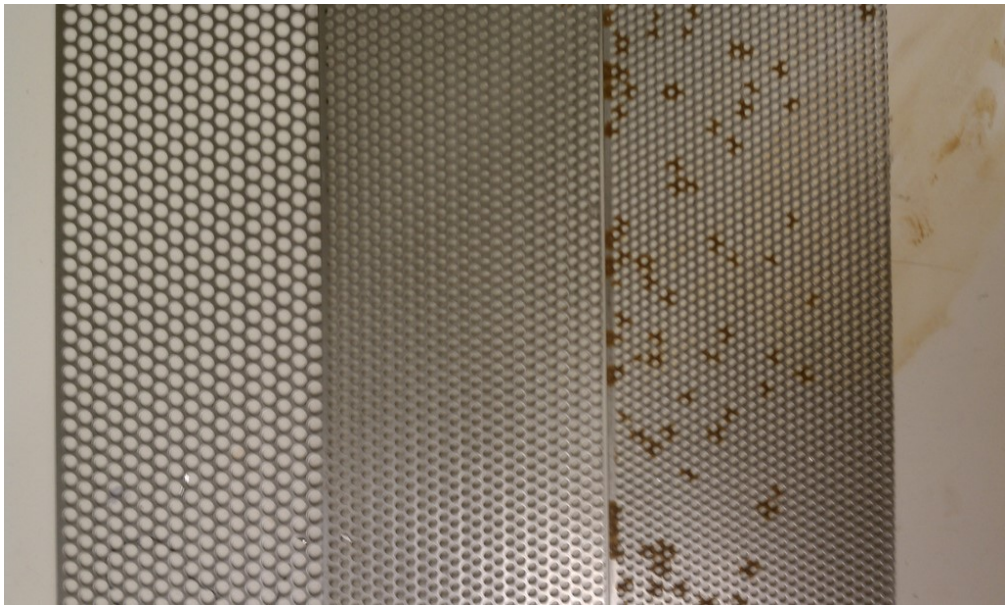

Fence models used for porosity studies (from left to right: 58% OA, 46%OA, 40%OA)

Our experiments showed that fences with lower porosity (more blockage) tend to reduce aerodynamic loads on heliostats, however the difference is not significant and probable not worth the extra cost. Lower porosity fences require more material to build and more substantial installations since they have to withstand much higher wind loads. Our flow visualization tests showed that a solid wall (a 0% porosity fence) was not effective at reducing flow velocity in a heliostat field and that a 40-50% open area (i.e. 50-60% blockage) fence seems to have a good amount of load-reducing capability. Here's one example to show the load reducing effect of fence blockage (~5x):

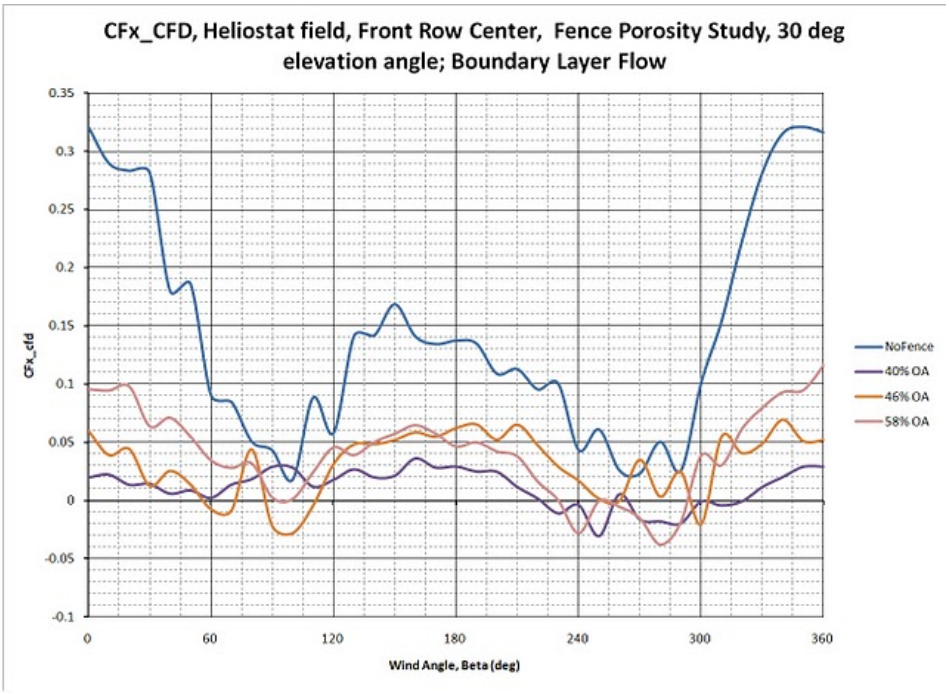

Plot of CFx (essentially drag) on a heliostat with fences of various open area with the "no fence"

case plotted as reference.

We found that a good fence height is, at minimum, as high as the highest point of the heliostat mirror when the mirror is at α=90°. For a 1m square mirror that has a minimum of 0.5m ground clearance, the fence height should be, at minimum, 1.5m. Fences that are significantly taller than that value don't seem to provide more beneficial load reduction.

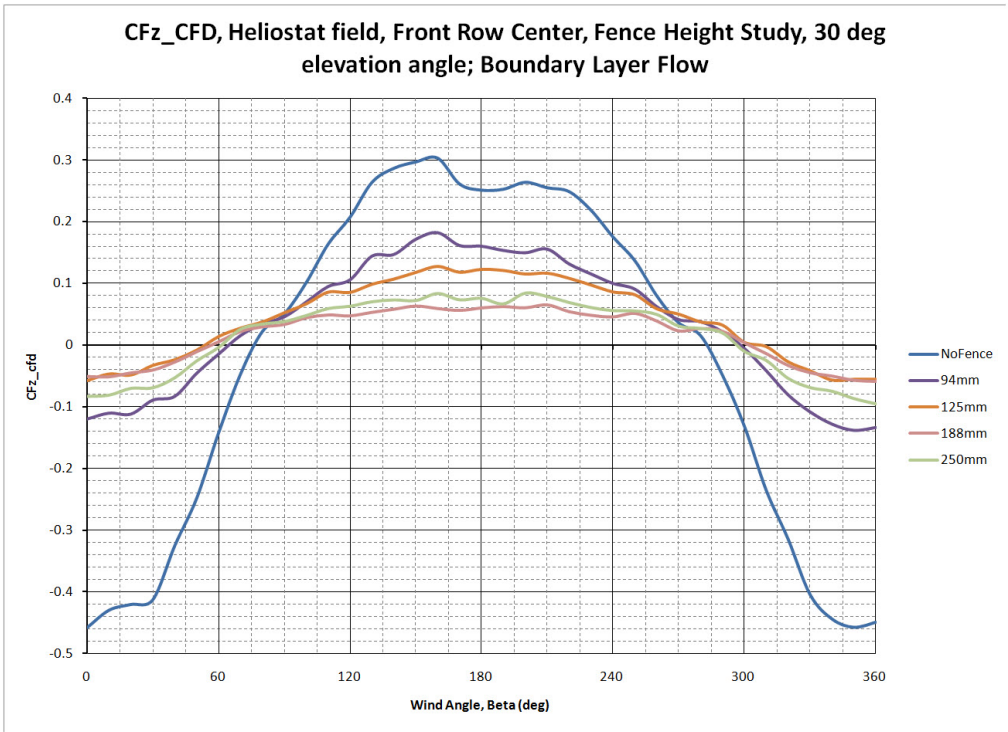

Plot of CFz (essentially lift) on a heliostat with fences of various heights with the "no fence" case plotted as reference.

We noticed during our flow visualization testing that multiple upstream fences appeared to have a qualitative effect in reducing local flow velocity in the heliostat field and almost "forcing" the flow stream above the heliostat field. We verified this in the wind tunnel by comparing the observed loads on a heliostat with no upstream fence, with a single upstream fence, and with multiple upstream fences.

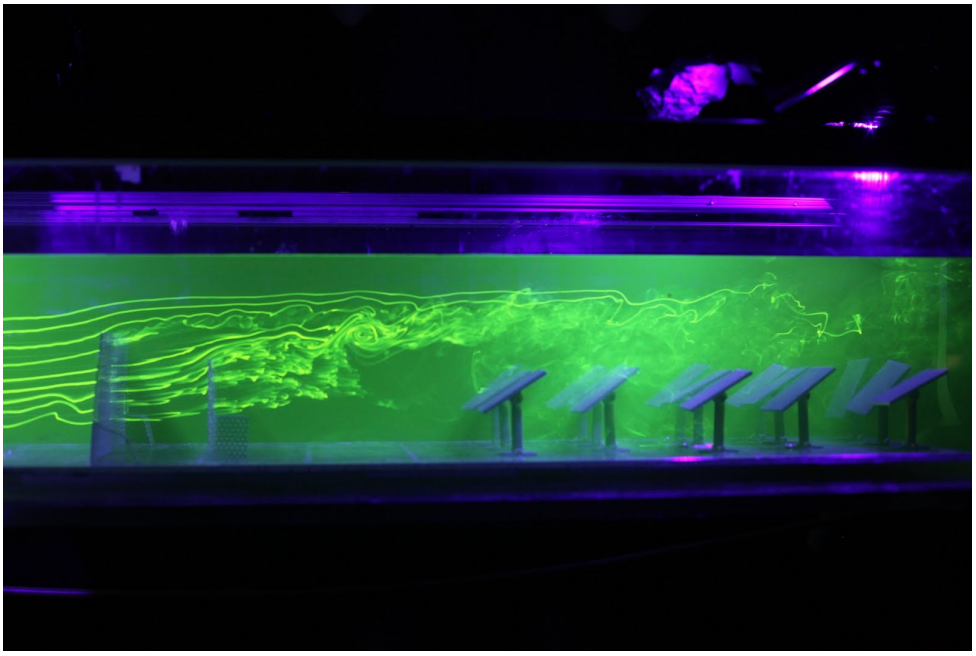

Multiple upstream fences, with shorter fence (1*Hmax) nearer the heliostat field. Both fences have 50% open area

A small fence (125mm tall, 1*Hmax) and a large fence (250mm tall, 2*Hmax) were used in the study with a 100mm x 100mm mirror and a heliostat centerline height of 75mm. This test also allowed us to examine the effect of fence upstream distance (6.6*H vs 10.4*H).

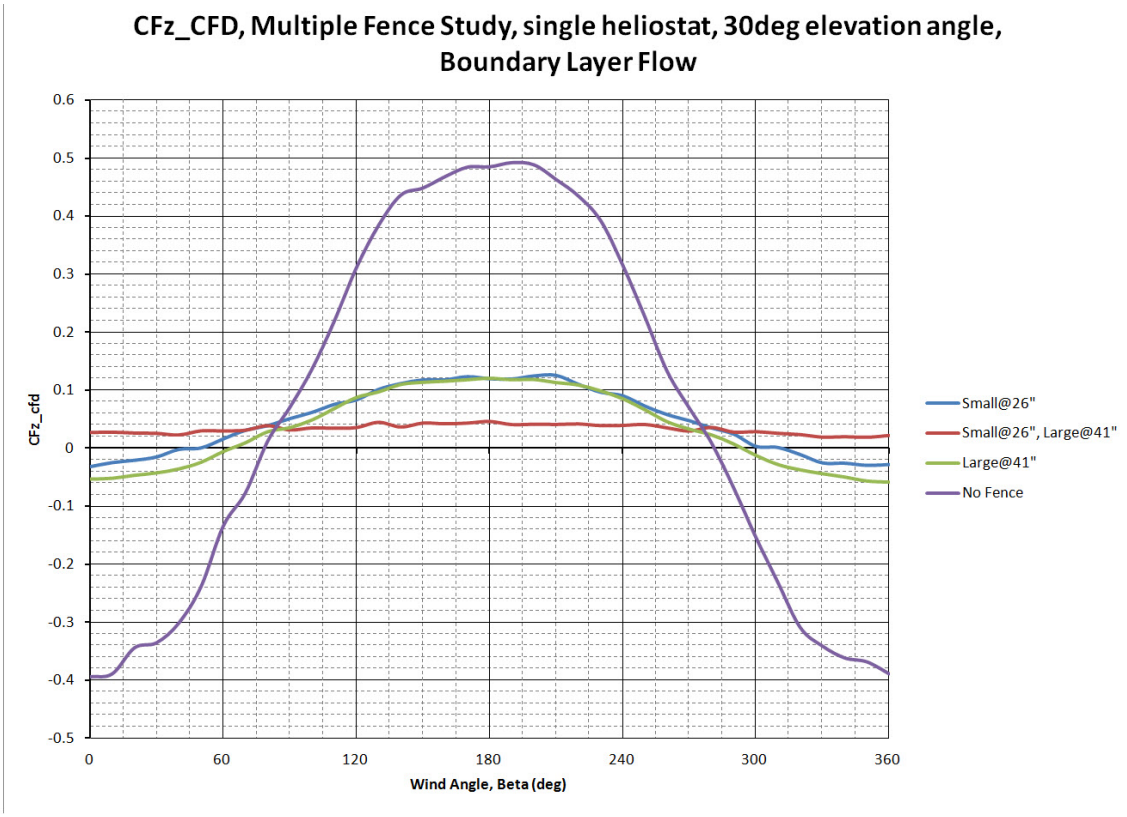

Plot of heliostat CFz (wind drag) with 0, 1 or several fences. Distances in legend refer to distance upstream of the instrumented heliostat.

We found that (in the case of CFz), a 2*Hmax tall fence, placed 10.4*H upstream of the heliostat has about the same effect as a 1*Hmax tall fence placed 6.6*H upstream of the heliostat. Therefore, if a single fence is being installed, costs would be reduced going with a smaller fence, closer to the heliostat field.

Also, multiple upstream fences have a noticeable impact in load reduction compared to a single fence. For example, in the case of CFz there is a 3x reduction in observed loads compared to a single fence, and a 10x reduction in loads compared to no fence. Of course, this comes at the added expense of a second perimeter fence.

To put some quick numbers behind each scenario, peak load coefficients are as follows (for a heliostat reflector at 30^{o} elevation):

Scenario	**CFz_peak**
No Fence	0.5
1*Hmax Fence @ 6.6*H upstream	0.12
2*Hmax Fence @ 10.4*H upstream	0.12
1*Hmax Fence @ 6.6*H + 2*Hmax Fence @ 10.4*H	0.04

Fence Costs

While the wind tunnel tests demonstrated aerodynamic load reduction using perimeter fences, it's important to examine the costs versus the benefits provided. Because the design and sizing of heliostats is driven by the aerodynamic loads, a reduction in these loads can lead to heliostat design requiring less material. Less material means a more flexible wind-resistant frame, smaller cable actuators to move the reflector and lower transportation and installation costs, all of which have a significant cost benefit. However, if the cost of installing a perimeter fence is high, it may offset any cost savings from the load reduction.

If we assume that CSP plants will be installed in fairly high volume and that the plants are each ~200MW in capacity, installing a single perimeter fence costs less than $\$1/m^2$ (meter squared of reflector area). At this cost, we feel that perimeter fences provide a very cost effective means of reducing heliostat aerodynamic loading and reducing overall plant cost.

Conclusions

While wind tunnel tests are not a replacement for real-world experiments and measurements, it is very valuable as an information source for estimating the general trends and approximate magnitudes of aerodynamic loads.

Through our wind tunnel experience we learned several critical items about heliostat fields:

- Densely packed fields provide increased sheltering for downstream heliostats, however this needs to be balanced against the risks of heliostat shadowing and blocking (see the Optical Simulation Code for one method of modeling this trade off).
- Using perimeter security fences to also act as a wind mitigation tool can have significant cost advantages on the overall system.
- Individual heliostat wind mitigations don't appear all that effective, especially considering the cost and material increase.
- Aerodynamic load conditions peak at different heliostat orientations, however a surprising number of these occur at elevation angles close to 30^{o} and 90^{o}.

We also learned a few things about wind tunnel testing during our set of experiments:

- It is hard to find and book wind tunnel time, adequate advance preparation is needed.
- Constructing robust models is worthwhile, because the downtime associated with repairing broken models can be significant. We suffered a model failure due to poor model construction that caused several days of downtime, which was not worth the savings from the rapid model fabrication
- Few things go "as planned" in a wind tunnel, and you must be prepared to improvise when the unexpected and unanticipated occurs (because it will).
- Build models as large as you can for the given wind tunnel; there will be less scaling errors.
- Coordinate transforms (i.e. putting your measured values into a new coordinate system) is not an easy task, and it's an easy place to make errors. Designing a model and data-logging system first to minimize any transforms is a good idea.

Areas for future work and deep dives include:

- We noticed a lot of noise in our load data from the heliostat field tests, which is probably from the small size of the models. Building a larger model field and testing in a wind tunnel capable of the larger models would be useful to get better data.
- We noticed a big discrepancy in the CMz coefficient of our single heliostat tests (small and large models), and it appeared that there was a ~10x difference between the two tests. We're not sure if this is real or some sort of unit conversion problem (in-lb vs. ft-lb).

Coefficient Summary and Reference

Load coefficients are dimensionless terms used to quickly compare the loading conditions for a specific object that allows the modification of environmental test conditions such as fluid speed and fluid density. They are a very useful way to examine loading conditions when the environmental conditions vary from one experiment to another. We wanted to provide the "Coefficient Quicklist" as a general, quick reference for anyone working in the area.

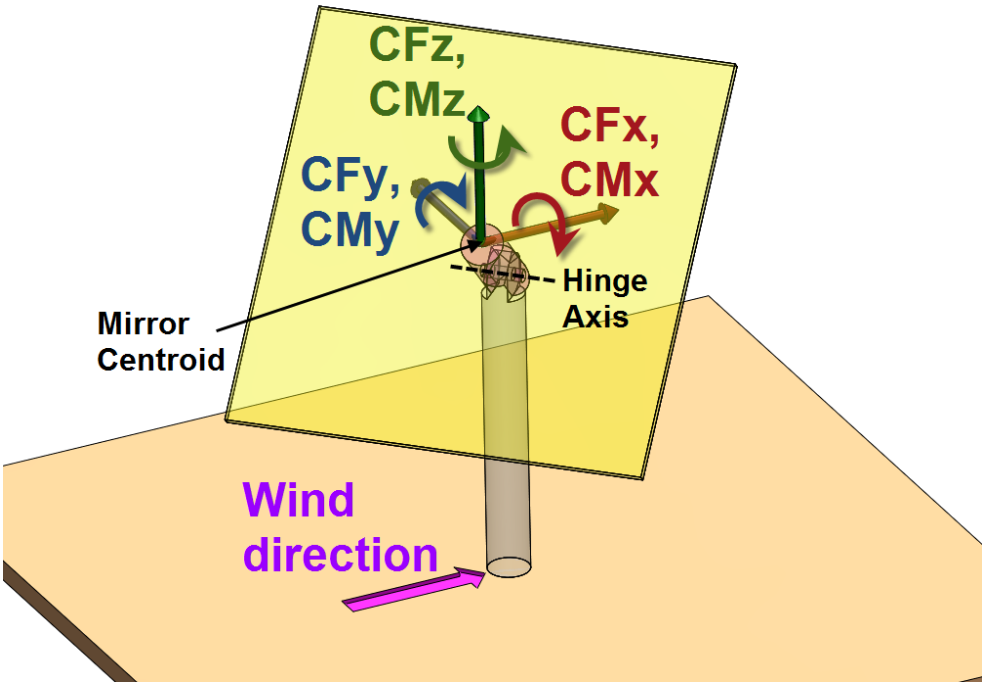

Coordinate system used, shown here at α = 45°, β = 45°

To convert from the reported coefficients into actual loads, we used the following equations:

$$F = C_f * \frac{1}{2} * \rho * V^2 * A \quad \text{(EQN 1)}$$

$$M = C_m * \frac{1}{2} * \rho * V^2 * A * L_{ref} \quad \text{(EQN 2)}$$

Where:

- $F\ (or\ M) =$ Force [N] or Moment [N-m]
- $C_f\ (or\ C_m) =$ Force or Moment coefficient (respectively)
- $\rho =$ Air density at given air temperature [kg/m3]
- $V =$ Air velocity (wind) [m/s]
- $A =$ Frontal Area [m2]
- $L_{ref} =$ Reference Length [m]

Isolated (or Edge) Heliostat

A heliostat that is not surrounded by other heliostats or structures, or, a heliostat that is at the edge of a heliostat field.

Maximum Load coefficients are as follows (atmospheric boundary layer conditions, TI = 14% @ HCL, data from 200mm x 200mm reflector tests):

CFx = 0.92 @ α= 90° and β= 0°
CFy = 0.72 @ α= 90° and β= 55° // **-0.72 @ α= 90° and β= 305°**
CFz = 0.60 @ α= 30° and β= 180° // **-0.68 @ α= 35° and β= 0°**
CMx = 0.15 @ α= 30° and β= 225° // **-0.15 @ α= 25° and β= 135°**
CMy = 0.10 @ α= 30° and β= 0° // **-0.15 @ α= 25° and β= 180°**
CMz = 0.01 @ α= 75° and β= 250° // **-0.01 @ α= 60° and β= 110°**

Non-Edge Heliostat

Non-edge heliostat is simply that, any heliostat that is not on the outer periphery of the field. Maximum Load coefficients are as follows[7] (atmospheric boundary layer conditions, TI = 13.2% @ HCL, data from 100mm x 100mm reflector field tests):

CFx = 0.28 @ α= 90° and β= 0°
CFy = 0.08 @ α= 90° and β= 55°
CFz = 0.25 @ α= 30° and β= 180°
CMx = 0.05 @ α= 30° and β= 225°
CMy = 0.03 @ α= 30° and β= 0°
CMz = 0.016 @ α= 90° and β= 250°

For the full set of results, see the Wind Tunnel Appendix.

[7] Load coefficients for non-edge heliostats are measured at the same α and β angles as edge heliostats, for comparison.